Smart Wireless Sensor System for Lifeline Health Monitoring under a Disaster Event

Sehwan Kim[1], Eunbae Yoon[1], Ting-Chou Chien[1], Hadil Mustafa[1],
Pai H. Chou[1,2], and Masanobu Shinozuka[1]

[1]University of California, Irvine, CA, USA and
[2]National Tsing Hua University, Hsinchu, Taiwan

ABSTRACT

This paper discusses issues of using wireless sensor systems to monitor structures and pipelines in the case of disastrous events. The platforms are deployed and monitored remotely on lifetime systems, such as underground water pipelines. Although similar systems have been proposed for monitoring seismic events and the structure health of bridges and buildings, several fundamental differences necessitate adaptation or redesign of the module. Specifically, rupture detection in water delivery networks must respond to higher frequency and wider bandwidth than those used in the monitoring of seismic events, structures, or bridges. The monitoring and detection algorithms can also impose a wide range of requirements on the fidelity of the acquired data and the flexibility of wireless communication technologies. We employ a non-invasive methodology based on MEMS accelerometers to identify the damage location and to estimate the extent of the damage. The key issues are low-noise power supply, noise floor of sensors, higher sampling rate, and the relationship among displacement, frequency, and acceleration.

Based on the mentioned methodology, PipeTECT, a smart wireless sensor platform was developed. The platform was validated on a bench-scale uniaxial shake table, a small-scale water pipe network, and portions of several regional water supply networks. The laboratory evaluation and the results obtained from a preliminary field deployment show that such key factors in the implementation are crucial to ensure high fidelity of the acquired data. This is expected to be helpful in the understanding of lifeline infrastructure behavior under disastrous events.

Keywords: Water pipe monitoring, MEMS sensors, ruptures, wireless sensor network

1. INTRODUCTION

The health of lifeline systems such as fresh water and sewage water pipelines is becoming a main concern in the United States and many parts of the world. Such infrastructure systems were built decades ago and are starting to show signs of age. Ruptures of water mains occur every day and cause property damages in addition to disrupting daily lives of millions. Early detection and preventive repair would be ideal but are not always possible. Therefore, real-time detection and timely damage control are the key to minimizing the adverse impact of such disaster events.

According to the web report of United Stated Geological Survey[1] (USGS), earthquakes have been occurring over ten times a year. Specifically in California, eleven earthquakes of magnitude 3 or greater occurs every week. Besides, as reported by the Environmental Protection Agency (EPA) update in 2010, much of the estimated 880,000 miles of drinking water infrastructure in the United States has been in service for decades and can be a significant source of water loss in the case of damage caused by natural disasters or deteriorating pipelines.[2] This report also states that water loss control and localization can effectively enable these agencies to maintain or increase revenue. As a result, the EPA introduced several detection and localization methods such as Magnetic Induction, Insertion Flow Meter, Inline Acoustic detection, etc. However, most of the introduced methods are not capable of real-time monitoring and detection, which can be crucial in most situations. Moreover, the above technologies are *invasive* in the sense that they require modifications to the pipeline systems, making them costly if not prohibitive especially on legacy systems.

This paper reports on the latest progress of a lifeline health monitoring system named PipeTECT. In this project, we build smart wireless sensor systems that can be deployed non-invasively on fresh water and sewage water pipelines.

Further author information: (Send correspondence to Pai H. Chou)
E-mail: phchou@uci.edu, Telephone: +1 949 824 3229

Multiple systems work together to collect acceleration data to be analyzed in the field or transmitted back to the laboratory in real time for post-processing. The ultimate goal is to build a SCADA, for supervisory control and data acquisition system capable of supporting real-time monitoring and real-time response to disaster events.

What makes such systems challenging are the quality of data sensing, timely and reliable communication from the field back to the laboratory, accurate analysis of collected data, and high power efficiency of the deployed system for extended operations with low maintenance cost. These problems are further exacerbated by the diverse deployment scenarios, which often create a harsh environment for wireless communication. Although it is possible to design a system that is optimized to each setting, it would be impractical and prohibitively costly. Instead, we aim to design one system that will be able to work well across the diverse operating conditions.

To address these challenging problems, we propose a vertically integrated solution with our PipeTECT design. At the hardware level, we choose the sensors, processors, and communication modules with the required performance, and we integrate them in a novel way to streamline their operation. We make our hardware expandable so that the data analysis can be done either on a daughter card in the field, or raw data can be logged on a memory card or transmitted back for processing in the laboratory. We design the communication module to be replaceable, so that different wireless modules can be swapped in based on the deployment site. An important but often overlooked feature is a flexible system management interface: that is, a tool that allows the user, not just the system designer, to control and configure the system in the most convenient way possible, whether they are in the field or in the laboratory.

This paper describes each of the subsystems of our PipeTECT SCADA design. We report experimental results from shake table tests as well as actual deployment of our system on a number of real-world lifeline systems, ranging from water pipes in manholes in a rural area to water pipes on a steel bridge. Finally, we report analysis results that quantify the accuracy of our sensing systems in the context of a blow-off test.

2. BACKGROUND

In our previous papers,[3,4] we described an earlier version of the PipeTECT wireless sensing system that was designed to monitor disastrous events. This section provides a background on the original PipeTECT system and a classification of the disastrous events under consideration.

2.1 Original PipeTECT System

The original PipeTECT system consists of two types of nodes: Gopher and Roocas. This organization enables the configuration to be adapted to the specific monitoring scenario.

A Gopher node contains the actual sensors such as accelerometers and the signal conditioning chip to digitize sensor data with a programmable band-pass filter. It sends the data to the local data aggregator for logging, processing, and transmission. Because RF transmission does not work well underground and due to the lack of power sources at most sensing locations (i.e., on the exterior of underground pipes), we choose the Controller Area Network (CAN) for providing the data link and power to the Gopher nodes over a wired interface. Multiple Gopher nodes can be daisy chained, and different Gophers may contain different sensing devices, such as camera modules, moisture sensors, gas sensors, etc.

A Roocas node is a data aggregator. It does not contain a sensing device; instead, it contains a CAN controller to get the sensing data from the Gopher nodes; it also powers all Gopher nodes on the attached CAN bus. Then, it has the options of (1) logging data to an on-board, removable Secure Digital (SD) flash memory card, (2) transmitting the data over one of the wireless interfaces, which may be Wi-Fi (by default), XBee (up to 1 km), XTend (up to 64 km). One limitation with the previous design was that the system was unable to meet the performance requirements, not to mention any local data processing, due to several bottlenecks in the system. These are the features that we improve in our latest design.

2.2 Disaster Events

Many types of disaster events can happen to lifeline systems. In particular, earthquake in densely populated areas such as California can cause damages to not only buildings and structures but also the associated lifeline systems. Multiple seismic data sets, during the 2005 Yucaipa, 2005 San Clemente, 2008 Chino Hills and 2009 Inglewood earthquakes were recorded by 31 accelerometers in CalIT2 building located on the University of California, Irvine campus.[5] From these earthquake data, we observe that the seismic frequency range is below 20 Hz. These recorded data allow us to distinguish earthquake

events from pipeline rupture events. The data would also be useful for synthesizing an earthquake event with a shake table for testing the PipeTECT system in the laboratory.

We focus on water pipelines, including fresh water and waste water under a disaster. Damages to these pipelines can be further divided into leakage vs. rupture. Leakage of fresh water does not necessarily translate into a disastrous event but may potentially cause severe property damages. On the other hand, leakage of waste water can cause contamination of the soil and the surrounding environment, which may be very costly to clean up. Various methods for leakage detection[6–8] have been proposed, but in general it is a difficult problem to locate the leak.

Our focus is on rupture events, which are characterized by the sudden, uncontrolled outburst of water, and they require immediate response. Unlike leakage, ruptures are highly disruptive as they prevent the normal operation of these lifeline systems. Moreover, the sheer volume of such an outburst is higher than leakage by several orders of magnitude and can cause a chain of damages to nearby structures that were never designed to withstand such unanticipated load in the first place. Contamination caused by such waste water will be even more difficult and costly to clean up. Therefore, we focus our effort on detecting, locating, and reacting to these rupture events in a timely manner.

2.3 Deployment Sites

We consider a variety of deployment sites that are representative of the diverse application requirements. The types of water pipelines that we monitor may be pressurized vs. gravity pulled; buried underground vs. above ground; accessible in a manhole, a pump station, a vault, or along another manmade structure such as a bridge; availability of utility power, energy harvesting, or battery. For the purpose of this study, we studied the following sites: Orange County Sanitation District (OCSD), Irvine Ranch Water District (IRWD), Santa Ana Watershed Project (SAWPA), and Vincent Thomas Bridge. Sec. 4 describes them in more detail.

2.4 Pipeline Monitoring

Different monitoring methods have been proposed. The intuitive way is to measure either the pressure or the flow with a pressure gauge or a flow meter as a direct way to infer rupture. However, unless the pipes have already been built with such a sensor during construction, retrofitting can be prohibitively expensive. Robots or mobile sensors[9] that flow with the water have also been proposed, but it is challenging to build devices that can operate in such harsh environments for extended periods of time while communicating reliably to the outside.

Our focus is on noninvasive monitoring. We propose to install accelerometers on the exterior of the pipes without invasive modifications to the pipes. The installation is relatively easy, as it entails mainly gluing the sensor (in our case, the Gopher node) to the pipe surface with a hot glue gun without compromising the structural integrity of the pipe. Other sensing modalities such as acoustic and microwave can also be incorporated later, but they are outside the scope of the current study. The goal of this work to quantitatively show that our proposed acceleration modality is suitable for rupture monitoring, and that the chosen sensor has the necessary sensitivity and specificity for this purpose when configured for the right sampling rate and bit resolution. Having raw data is insufficient, but additional processing is required. One other goal of this work is to determine the complexity of the processing algorithms required so that we can select the right processing elements to install in the field in order to work with the limited, costly communication bandwidth back to the laboratory.

3. SUPERVISORY CONTROL AND DATA ACQUISITION (SCADA) SYSTEM

Our previous paper[3] reported mainly on the sensing and data aggregation *nodes* (namely Gopher and Roocas). However, our proposed PipeTECT system actually includes not only a network of such nodes but also the entire SCADA, i.e., the command center that can display and disseminate data from all the sensors, performs processing, and issue commands for remedial actions if necessary. This section describes the new features that have been added to the nodes and to the entire SCADA since our last paper.

3.1 Sensing Subsystem

We implemented a number of enhancements in the sensing system, namely the Gopher node. First is a significant improvement in the sampling rate. Second is an efficient use of the signal conditioning chip by achieving a stable sampling rate of over 1000 samples per second. As a parallel effort to ours, a platform based on the iMote2 and the ISM400 (formerly SHM-A) sensor module was promoted by researchers from the ISHMP group at University of Illinois at Urbana-Champaign (UIUC) on structural health monitoring of civil infrastructure systems, henceforth referred to as the ISHMP platform.[10] It is composed of the iMote2 node designed by Intel and distributed by Crossbow, connected to ISM400 board designed and distributed by UIUC. The ISM400 board is custom designed to be plugged into the iMote2's expansion connector. ISM400 uses the ST Microelectronics LIS344ALH accelerometer, a consumer-grade accelerometer that retails at $5-6 a piece. Gopher contains one, two, or three SD1221L-002 uniaxial accelerometers (one on-board, plus two vertically mounted removable PCBs) that sell for $160-180 per axis. A recent study shows that LIS344ALH can pick up acceleration as low as 0.5 Hz on the Jindo Bridge in Korea.[11]

Note that water pipe monitoring is a very different application from structural health monitoring. SHM for bridges and buildings often require sensitivity to low frequencies in the regime of 0.5 Hz, but water pipe monitoring requires sensitivity to the 30-300 Hz range. We are interested in finding out how the ISM400 and Gopher sensors would perform in the two applications. Section 5.1 shows their results.

3.2 Data Aggregation and Relay

We addressed a number of bottlenecks in data logging bandwidth and wireless transmission. To overcome the data logging speed limitation, we implemented a number of enhancements, including streamlined data transfer to the memory card for the file system and streamlined data transmission. To enable transmission over a longer distance, we experimented with both a powerful antenna and relaying using Wi-Fi base stations in WDS mode. The powerful antenna is one mounted on a pole and requires a power source of 24V DC. The reason for choosing a powered, omnidirectional antenna as opposed to a directional antenna is that although a directional antenna can be more energy efficient, it can be very sensitive to the exact direction. Any slight change in the direction can actually cause the system to lose connection completely. Therefore, an omnidirectional, powered antenna can be more practical for the purpose of a data aggregator or a relay unit. We have conducted a number of tests on the transmission range on campus. It was possible to achieve over 1 km distance with a very high packet delivery rate.

However, because the antenna must be powered by a high-voltage (24V) and the antenna on the pole is bulky, it can actually become very difficult and dangerous to deploy, especially in the case of Vincent Thomas Bridge. It can be quite windy on the bridge, making it difficult to carry the heavy antenna pole and battery to the deployment location. Moreover, the antenna proved to be very bulky on the narrow metal walkways underneath the bridge. Therefore, the preferred solution is to deploy a number of relays. All of our chosen RF transceivers, including XBee, XTend, and Wi-Fi support relaying with their protocol stacks. In the case of Wi-Fi, the base stations can be configured in WDS (wireless distribution system) mode. We configure a number of access points (AP) to work as relays, so that all nodes can connect to any of the relay base stations or the main base station and form one network.

3.3 System Server

We have the option of connecting the main AP to a wired Ethernet uplink or connecting the relay base stations to a mobile Wi-Fi hotspot, which provides an Internet connection over the 3G or 4G cellular data network. An initial version of the server can receive and render incoming data as a dynamic web page. Multiple Roocas nodes can aggregate data from multiple Gopher nodes, where each Gopher node can provide up to 3 channels of acceleration reading (X, Y, Z axes). At the network level, each Roocas node provides a data stream that can encapsulate several sensing channels. The server saves each data stream in a common data storage for later use. Once the readings are saved correctly, we can do further data processing, which may include FFT or wavelet decomposition and various filters. The results are then rendered for display as a web page. The server currently works as follows. On starting up, it listens for the *heart beat messages* from Roocas nodes. Upon receiving a heart beat message, the server creates a data entry in the data storage. Then, the server replies with a START command to the Roocas node to start sensing and transmitting the data back to the server. At the same time, the web graphic generating program is running as another daemon process. It fetches readings from the data storage and renders the graphs. Live pictures are generated every 500 ms, while the associated web page is refreshed every 3 seconds automatically. These intervals are selected based on the latency of rendering the graphs and based on the average

(a) Shake Table Setup (b) ISHMP platform (c) iGopher

Figure 1. The Shake Table Test Setup for iGopher and ISHMP platform

browser refresh rate. Although many features are still needed, our current version represents a foundation upon which the envisioned SCADA can be built.

3.4 Statistical Data Processing for Rupture Detection

Time domain analysis is a simple way to detect and identify rupture events with low computational complexity. A rupture event is always accompanied by a sharp change in the acceleration. Thus, simple computing the local maxima of the acceleration gradient values can be located the damage location. In addition, there are three more time domain analysis approaches: Running Variance, Windowed gradients, and Max-Min difference. However, in time domain analysis, it is not always possible to distinguish rupture or leakage event from ground acceleration if the magnitude of the rupture or leakage event is small.

In this case, frequency domain analysis such as Fast Fourier Transform (FFT) and Power Spectral Density (PSD) would be useful to detect or identify the small amplitude of a rupture event. However, this frequency domain analysis does not include time history information. Therefore, we introduce time-frequency analysis such as STFT technique and wavelet transformation. These two analysis methods are reliable, adaptable, and commonly used for signal analysis. Furthermore, local processing by these kinds of statistical data analyses is required to reduce the amount of the transmitted data. It would be also helpful in improving the power management.

4. EXPERIMENTAL SETTINGS

We conducted experiments in several different experimental settings, both in the laboratory and in the field. We briefly describe each experimental setting.

4.1 Shake Table

We used a shake table to evaluate the performance of sensors under the simulations of ground acceleration, pipeline vibration, and dynamic response of civil structures. The test motion was synthesized by an APS 400 Electromagnetic Shaker and HP 35670A dynamic signal generator. Note that rupture detection in a water pipe network must respond to higher frequencies compared to those of seismic events, structures, and bridge as mentioned in Sec. 3.1. Such sensors should be designed to have a wide measurement bandwidth, so that they can be applied to monitoring a wide variety of civil structures.

To validate the performance of our sensing subsystem, we adapted a version of Gopher by adding the same iMote2 connector as the ISM400 board, so that it can be plugged into the iMote2. This iMote2-Gopher combination is named iGopher, as shown in Fig. 1(c). We evaluate it against the ISHMP platform (iMote2+ISM400) as shown in Fig. 1(b) using a shake table. Since the ISHMP firmware for iMote2 has a limitation of memory to store the measured data, the ISHMP platform cannot handle data streaming in real-time monitoring fashion. Thus, the ISHMP platform was operated to transmit the data by three steps: sense, store, and transmit, whereas the Gopher can transmit the data sampled by MEMS sensor in real time manner to a nearby Roocas unit. We secured both the ISHMP node and iGopher on the same shake table with hot glue, the same as what we would do on a water pipe. Section 5.1 presents the experimental results.

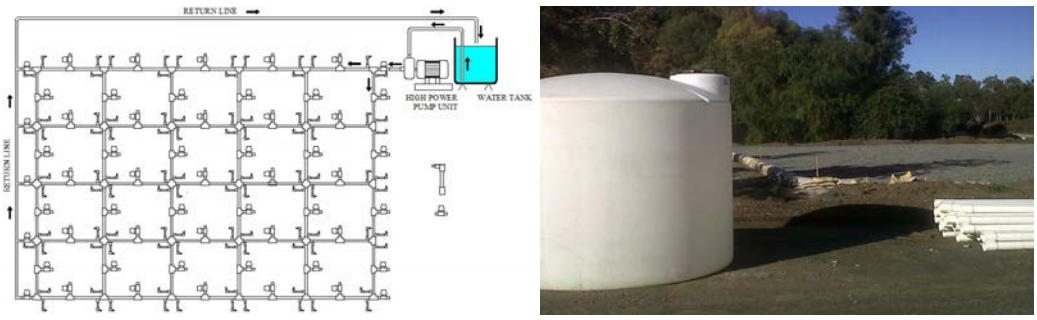

(a) Drawing of a 4-inch Water Pipe Network (b) Photo of Rattlesnake Reservoir

Figure 2. Small-Scale Water Pipe Network at IRWD

(a) SARI Sheet 11 (b) Airvac 340 (c) Blowoff Valve 0335

Figure 3. The Gravity Water Pipes at SAWPA

4.2 Small-scale Water Pipe Network Model

An advanced small-scale water pipe network was constructed at Rattlesnake Reservoir as shown in Fig. 2. In developing the advanced design of this pipe network, we considered experimental results from previous lab-based water pipe network.[3] While the most common pipes are of 8-inch diameter, our initial study utilizes 4-inch ones to reduce the overall water and pressure requirements. Fig. 2(a) show the drawing of the 4-inch PVC (polyvinyl chloride) small-scale pipe network. By the introduction of transducers, we captured the steady-state behavior and the presence of remotely operated ball valves to open, close, and vary the degree of fluid moving through a given pipe section. These electronic solenoid control valves simulated different damage scenarios covering small pipe leakage to a major line rupture. These simulated events were controlled remotely, not manually. In addition, for steady-state pressure at entire water pipe network, a high-power pump unit and water tank were adopted.

4.3 Gravity Pipes

Two partners have *gravity-pulled* pipes. First, the Santa Ana Watershed Project Authority (SAWPA) has PVC hydraulic head gradient pipelines by gravity. A waste water pipe can be accessed via either an *airvac* or a *blowoff valve*. The former is for release of waste air and is located at a relatively higher elevation than the latter, which is for release of waste water. Fig. 3(a) shows manholes AV 340 (an airvac) and BO 0335 (a blowoff valve) selected for the field test. A blowoff test entailed measuring vibration at an airvac (Fig. 3(b)) while directing waste water from a blowoff valve into a 5000-gallon tank (Fig. 3). Second, with Irvine Ranch Water District (IRWD), we also tested a section of a gravity pipe from Irvine Lake (upstream) to Rattlesnake Reservoir (downstream). Rupture was simulated by opening a control valve of a metal pipeline system. As shown in Fig. 4, most parts of the pipe were underground but the instrumented section was above ground. A pressure gauge had already been installed in this section, which enabled us to correlate vibration with pressure change. Three Gophers were deployed at i) upstream 7m away from the control valve, ii) upstream near the control valve, and iii) downstream near the control valve, as shown in Fig. 4. The Gopher measured the acceleration change in vertical direction. The sampling frequency was set as 1 ksps. The Nyquist frequency (500Hz) was thought to be enough to cover dominant frequency ranges of metal pipes. The water pressure upstream (Gopher#2 in Fig. 4) dropped from 197 psi before the valve opening to 175 psi after opening and remained nearly constant during the full open state, and then it returned to the original

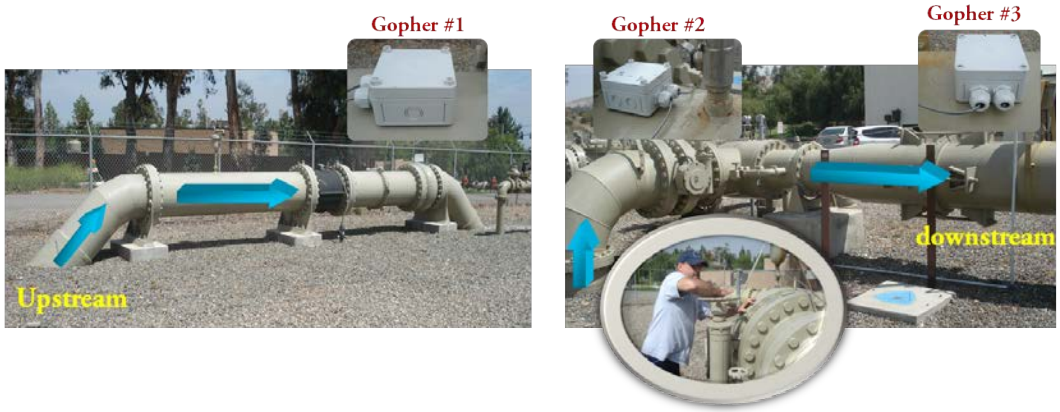

Figure 4. Experimental Setup Showing IRWD Metal Water Pipe

(a) Pump Station at OCSD (b) Vault Site at OCSD

Figure 5. Pressurized Water Pipes at OCSD

pressure value after closing the valve. Unlike upstream pressure, the water pressure downstream remained at around 48 psi during the whole test.

4.4 Pressurized waste water pipes

The Vault by the Bay Bridge and the Bay Bridge Pump Station of the Orange County Sanitation District (OCSD) have been surveyed as deployment sites for analysis of pressurized sewage pipes. Differing from gravity water pipes, the pump station as shown in Fig. 5(a) pumps sewage out of a well when it exceeds a certain level. Another difference is that this site uses metal pipes rather than PVC. Also, this site has utility power and is furnished with a DSL line for Internet connection. Fig. 5(b) shows a vault that is 500 m away from the pump station. Sewage from the pump station is split into two pipes that run along the street towards the treatment plant.

The Vincent Thomas Bridge is a suspension bridge located at the Long Beach harbor as shown in Fig. 6. It is over 1.8 km in total length, with a main span of 457 m. Since this is a metal bridge, and there are various vibration excitation sources due to traffic loads, wind, and water flow, this bridge is selected as the test bed to evaluate the performance of wireless smart sensors and network topology for relay. In general, the natural frequency of bridge is below 5 Hz, while that of water pipe is hundreds of Hz. Hence, this site has motivated us to validate the performance of PipeTECT system.

5. RESULTS AND ANALYSIS

5.1 Shake Table

The collected power spectral density (PSD) data was analyzed to examine the natural frequency response of the MEMS sensors. We used 1024 PSD data points sampled at 1000 samples/sec. Leakage was handled by a smoothing technique using standard spectral window function such as Hanning window. We focus on the noise floor in the low frequency range with a small displacement. The shake table was controlled by a function generator programmed for 0.1Hz, 0.5Hz, and 1Hz

(a) Deployment at Vincent Thomas Bridge (b) Vincent Thomas Bridge

Figure 6. Pressurized Water Pipes at Vincent Thomas Bridge

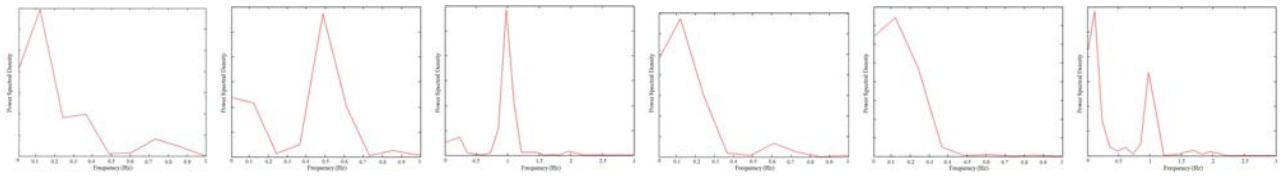

(a) iGopher@0.1Hz (b) iGopher@0.5Hz (c) iGopher@1.0Hz (d) ISHMP@0.1Hz (e) ISHMP@0.5Hz (f) ISHMP@1.0Hz

Figure 7. Frequency Domain Analysis of iGopher and ISHMP platform

with 1mV displacement. Fig. 7 shows the frequency-domain PSD for iGopher and the ISHMP (with ISM400) platform over these frequencies.

Our iGopher correctly captured the peaks at 0.1Hz, 0.5Hz, and 1Hz as expected. This study also shows that the ISM400 board is not necessarily responding to the 0.1 Hz frequency as previously reported from the Jindo Bridge study. Our data shows that it may have the *sensitivity* but not the *specificity* needed. As a suspension bridge, the Jindo Bridge has a displacement as high as 12 cm when the 0.1 Hz frequency is measured. Therefore, for all practical purposes, it can be considered to be almost like a DC value, and virtually all accelerometers can pick up such low frequency. However, when the displacement is sub-millimeter as is the case of concrete structures or water pipes, then the ISM400 is unlikely to detect such low frequency components due to its relatively high noise floor. The noise floor of our Gopher sensor is lower than that of the ISM400 by an order of magnitude when below 1 Hz frequency. Thus, we deem the iGopher suitable for both water pipe monitoring and structural health monitoring applications.

5.2 SAWPA

Fig. 8(a) shows the entire time history of PipeTECT system at Airvac 340. The start and end times of the blowoff are marked with dotted red lines on the figures. Figs. 8(b), (c), and (d) show pre-blowoff (0-650 sec), blowoff (650-1160 sec), and post-blowoff (1160-1515 sec), respectively. In time domain, it is not always possible to distinguish between an earthquake event or ambient noise by just looking at a sudden change of the signal. It can be attributed to the potentially small amplitude of vibration and to high damping effect of PVC pipes, as previous research reported. In frequency domain, on the other hand, the frequency content of the signal related to a rupture event can be precisely detected. Fig. 8 shows that the range of 30-50 Hz is related to the blow-off frequency, since it peaked during the blowoff but is lower before and after, relative to the 60 Hz electric noise, which remains constant.

5.3 IRWD

In this experiment, initially, the valve was fully closed (0-205 sec) and then began to open (indicated as B.O in Fig. 9(a)). The valve was fully open from 375-915 sec (F.O) for 540 seconds. Then, it began to close at 915 sec (B.C) and was fully closed at 1105 sec. The time history of the change in acceleration at the Gopher location 1 during the first valve transition (205 to 375 sec) had the peak of acceleration around two times greater than that of the closed state. However, the sudden change in acceleration does not happen during the closing valve operation period (915 to 1105 sec), during which the water pressure recovered to the original value. Fig. 9(b) shows the converted frequency content, which shows a spike near 300Hz, which we attribute to the simulated rupture event. Compared to the 30-50Hz range at SAWPA, the metal pipe at IRWD showed a much faster speed of impact wave propagation. Fig. 9(c) shows the STFT result of measured data by Gopher

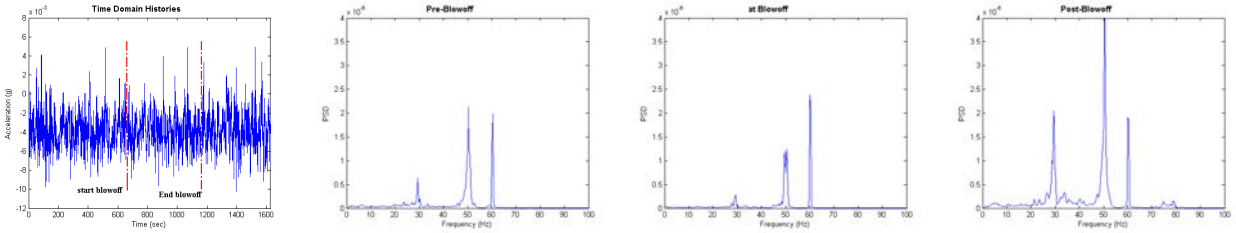

(a) Entire time history (b) Pre-blowoff (c) Blowoff (d) Post-blowoff

Figure 8. Data Analysis of PipeTECT Sensor@SAWPA

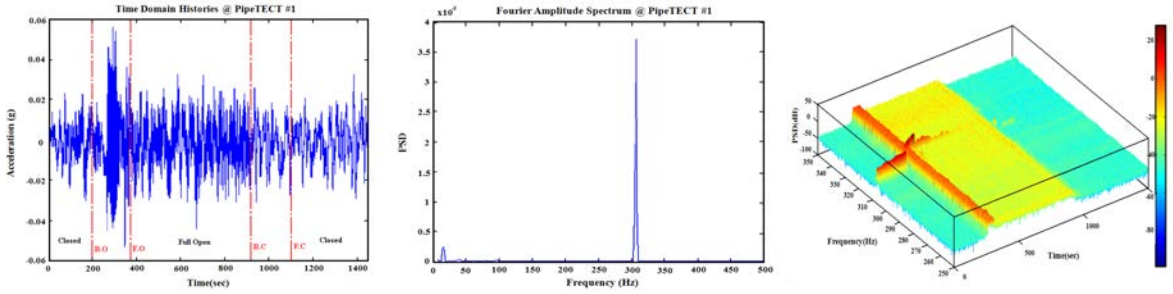

(a) Time history (b) Frequency domain (c) STFT analysis

Figure 9. Data Analysis of PipeTECT #1 at IRWD

1 for time-frequency analysis, where the time window length for the STFT was taken as about 4,096 data points with the overlap ratio of 0.5. This analysis reveals that the dominant frequency before the valve opening was 306 Hz and shifted to around 315 Hz during the valve transition. After the valve closing, it returned to the original frequency. In this case, the pressure drop was also identified in the frequency domain. In time domain, the results show that a sharp change in the water pressure is always accompanied by a sharp change in the acceleration on the pipe surface at the corresponding location along the pipe. Besides, in SFTF analysis, this rupture event is also observed through frequency shift.

5.4 Vincent Thomas Bridge

For the Vincent Thomas Bridge, we experimented with wavelet analysis, a relatively new and promising technique in data processing and signal analysis for its ability to maintain localized characteristics in both time and frequency domains. Fig. 6 shows the deployment of PipeTECT sensing system on the Vincent Thomas Bridge. Wavelet Transform decomposes the signal into components called wavelets containing information extracted from the original signal. Examining the decomposed wavelet can identify the local features of the signal. The major advantage of wavelet analysis lies in its ability to examine the data without losing the time component. We apply wavelet decomposition to the data collected from three PipeTECT sensing system installed on the Vincent Thomas Bridge. Discrete wavelet transform (DWT) was chosen for its low complexity, making it suitable for in-field processing.[12] The DWT analyzes the signal by passing it through a filter of different frequencies determined by the level of decomposition and focuses on a specific span of time at each decomposition level. At the end of the process, the original signal will be decomposed into a number of components, each representing a frequency band and time period. As a result, the signal can be expressed in two parts, wavelet details and approximations, as follows:[13]

$$f(t) = \sum_{i=1}^{i-j} D_i(t) + A_j(t) \tag{1}$$

where $D(t)$ is the wavelet detail and $A_j(t)$ stands for the wavelet approximation of the j^{th} level. Fig. 10 shows a graphical representation of DWT tree. Damage is often detectable as deviation from natural frequencies. We first decompose the vibration signal using Daubechies wavelet (DB) function and a 4-scale multi-resolution analysis. Fig. 11 illustrates the details of signals d1-d4 and the evolved a4 signal on PipeTECT2. Second, we apply a threshold filter on the vibration signal to separate the high-frequency component of low interest (mainly noise) from the low-frequency signal with higher

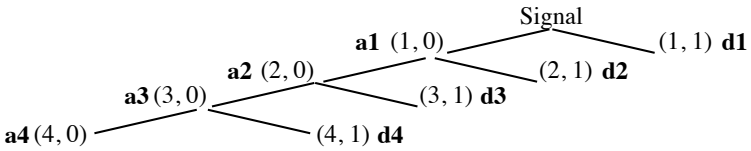

Figure 10. Wavelet Tree

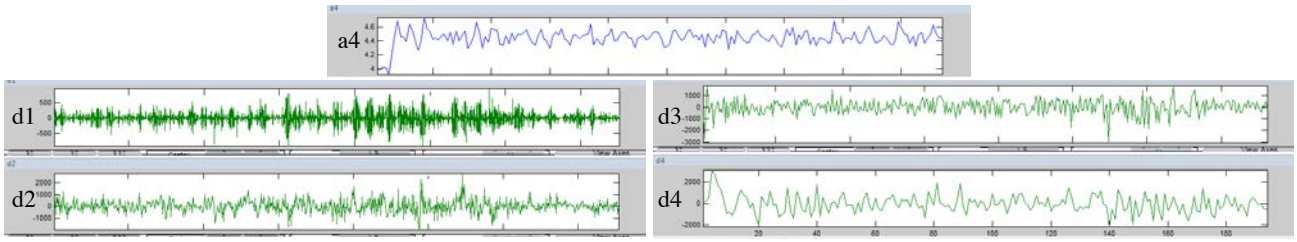

Figure 11. Decomposition of the vibration signal at PipeTECT2

amplitude indicating important changes in the state of the structure. The reconstructed signal after filtering will contain only the low-frequency signal while maintaining the original features of the vibration signals. Figs. 12(a) and 12(b) show the original and reconstructed signal after filtering.

The DB wavelet transform using discrete convolution can be performed on embedded processors due to its low complexity. A future expansion of the present board using a dual-core MCU with floating point units for data processing purpose on an expansion card over SPI[14] will be implemented in our future work.

6. WIRELESS COMMUNICATION

We tested multiple Roocas nodes on a Wi-Fi network for real-time data aggregation at locations above, but here we report the results from the UCI campus and on the Vincent Thomas Bridge. We have two options to build networks for Roocas units: to use powerful radios and antennas, or to use WDS enabled access points.

6.1 UCI campus: Extended Star vs. Multi-Hop Topologies

We assessed the performance of the long range wireless communication network formed with Cisco Aironet 1300 APs shown in Fig. 13(a). It was chosen for its ability to act as a repeater for relaying packets and for runtime configuration capabilities. We equipped it with a 4-foot-long omnidirectional high-gain antennas and drove it with high transmission power. Two different topologies were tested: extended star and (linear) multi-hop. Fig. 13(b) shows the three selected locations on UC Irvine campus: Engineering Tower (ET), Engineering Parking Structure (EPS), and Green Bridge (GB). In both topologies, the host PC and the main AP were both located at the top of ET. In case of *extended star* topology, the repeaters were at EPS and GB, and both repeaters were directly associated with the AP but not each other. On the other hand, in *multi-hop* topology, the EPS repeater became a relay for the GB repeater. In both cases, the PipeTECT sensing system was associated with its nearest repeater (at EPS and at GB), which forwarded data to the AP, through a

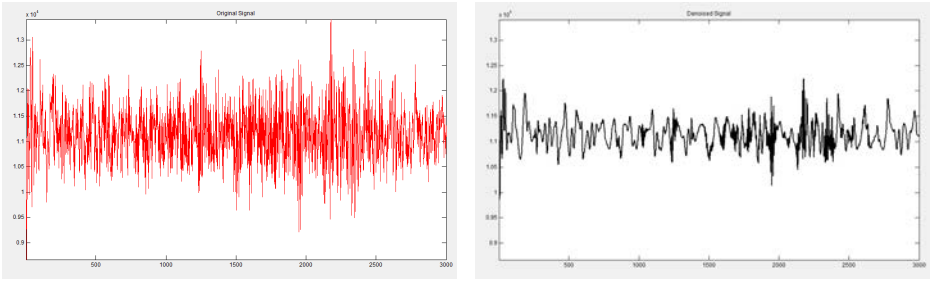

(a) (b)

Figure 12. (a) Decomposition of the vibration signal at PipeTECT2, (b) at PipeTECT3.

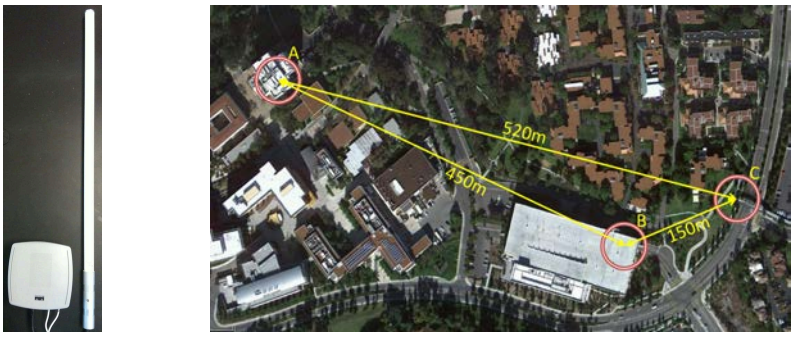

(a) (b)

Figure 13. (a) A Cisco Aironet 1300 access point (AP) and a high-gain omnidirectional antenna; (b) Locations of APs and repeaters: A. Engineering Tower (ET), B. Engineering Parking Structure (EPS), C. Green Bridge (GB).

Table 1. Round trip time and Packet Transfer Performance on UCI Campus

	Round-trip time (ms)			Extended Star			Multi-Hop		
Device	Min	Max	Avg.	#Tx Recs	#Rx Recs	Drop Rate	#Tx Recs	#Rx Recs	Drop Rate
Repeater1	2	57	9						
Repeater2 (AP associated)	2	35	8						
Repeater2 (Relayed)	4	25	9						
PipeTECT at EPS	14	67	48	135,405	135,153	0.2%	388,526	386,123	0.6%
PipeTECT at GB	7	96	21	103,738	100,001	3.6%	355,808	352,515	0.9%

relay if necessary. Each PipeTECT transmitted 1000 records per second, and the AP and repeaters were configured for 1-2 Mbps bandwidth and WiFi Protected Access (WPA2). The host PC sent a PING request and measured the delay of PING response from the target device.

Note that the response time and packet transfer performance depend very much on the channel condition, which depends on the number of hops, communication distance, and external interference. In addition, the internal antenna used in the sensor nodes further contributed to response time variations due to the relatively low gain. In contrast, the repeaters have less variation due to the higher gain. Multi-hopping topology showed higher packet drop rate and longer response time, but it can effectively extend the communication distance. We are currently evaluating bridge-to-bridges configuration to replace the repeater as an alternative way to extend the communication distance without losing bandwidth capability, though it costs more.

6.2 Vincent Thomas Bridge

Vincent Thomas Bridge posed a number of challenges. First, the space constraint did not allow large antennas to be installed, and relaying was the only option. Second, the metal structure made it difficult to find the optimal topology. Even without space constraint, the shape of the bridge would block the line of sight from one end to the other end of the bridge. We used WDS-enabled APs to compose a wireless backbone network for PipeTECT. However, the bandwidth became narrower as the number of hops increased. Therefore, high throughput was essential. We formed the multi-hop network with five, 100-meter apart, Buffalo WHR-HP-G300N 802.11n routers capable of 150 Mbps throughput with relatively small and light antennas and enclosures.

Given a number of simultaneous transmissions, increasing the number of hops apparently increases the drop rate. However, the drop rate was affected more by the number of simultaneously transmitted packets than by the number of hops. This can be observed from PipeTECT2, which takes fewer hops than PipeTECT3 does but suffers from more dropped records, mainly due to more relaying traffic by PipeTECT2.

7. CONCLUSIONS AND FUTURE WORK

We have described the latest development of the PipeTECT system, including Gopher sensing nodes and Roocas data aggregators. They achieved significantly higher sampling rates ($\geq$1000 Hz) with simultaneous data logging and data transmission with a higher power efficiency. We compared our sensing results with those of another widely used platform

(a) WDS Router installed (b) Roocas powered by a lantern battery (c) Gopher attached on the water pipe along the bridge

Figure 14. Metal structures of Vincent Thomas Bridge

Table 2. Response Time and Packet Transfer Performance on Vincent Thomas Bridge

	Round-trip time (ms)			Multi-hop		
Device	Min	Max	Average	#Tx Recs	#Rx Recs	Drop rate
Router1	2	14	8			
Router2	4	35	9			
Router3	4	57	13			
Router4	7	34	14			
Router5	9	48	17			
PipeTECT1	10	25	15	649,580	648,315	0.19%
PipeTECT2	13	40	19	639,192	636,272	0.45%
PipeTECT3	15	45	21	626,261	624,047	0.35%

based on the ISM400 for structural health monitoring. Results showed that our Gopher sensor have a lower noise floor by an order of magnitude and a wide frequency response range that covers not only water pipe monitoring but also structural health monitoring. Our network and server architecture prototype was operational for real-time data upload, viewing, and control over the Internet. We validated our system in a number tests, including both miniature-scale pipelines and a variety of actual field deployments on different types of water pipes. Our initial results appear promising as the first step towards a scalable, real-time SCADA for lifeline systems.

ACKNOWLEDGMENTS

This study was done under a National Institute of Standards and Technology (NIST) Technology Innovation Program (TIP) Grant 080058, as a joint venture with the Orange County Sanitation District (OCSD), Irvine Ranch Water District (IRWD), Santa Ana Watershed Project Authority (SAWPA), and Earth Mechanics, Inc. The authors also acknowledge assistance from MarcoPolo Velasco, Carlos Quintero, Sergio Carnalla, Sungchi Lee, Debasis Karmakar, Sudib Mishra, Chih-Wei Huang, and Jamie Robertson. Their support is immensely appreciated. This work is also sponsored in part by National Science grants CMMI-0826639, CNS-0448668, CNS-0721926, and CBET-0933694. Any opinions, findings, and conclusions or recommendations expressed in this material are those of the authors and do not necessarily reflect the views of the National Science Foundation.

REFERENCES

[1] USGS (United Stated Geological Survey), "Historic united states earthquakes." http://earthquake.usgs.gov/earthquakes/states/historical.php/ (November 2009).

[2] EPA (Environmental Protection Agency), "Control and mitigation of drinking water losses in distribution systems." EPA 816-R-10-019 (November 2010).

[3] Shinozuka, M., Kim, S., Chou, P. H., Fei, L., and Kim, H. R., "Nondestructive monitoring of a pipe network using a mems-based wireless network," in [*Nondestructive Characterization for Composite Materials, Aerospace Engineering, Civil Infrastructure, and Homeland Security IV*], (March 9 2010).

[4] Shinozuka, M., Karmakar, D., Chou, P. H., Kim, S., Kim, H. R., and Fei, L., "Non-invasive acceleration-based methodology for damage detection and assessment of water distribution systems," *Smart Structures and Systems* **6** (July-August 2010).

[5] Ulusoy, H. S., Feng, M. Q., and Fanning, P. J., "System identification of a building from multiple seismic records," *Earthquake Engineering and Structural Dynamics* (September 22 2010).

[6] Hunaidi, O. and Giamou, P., "Ground-penetrating radar for detection of leaks in buried plastic water distribution pipes," in [*Proc. 7th Int. Conf. on Ground Penetrating Radar*], (1998).

[7] Hunaidi, O. and Chu, W. T., "Acoustical characteristics of leak signals in plastic water distribution pipes," *Journal of Applied Acoustics* **58**, 235–254 (February 1999).

[8] Hunaidi, O., Wing Chu, A. W., and Guan, W., "Leak detection methods for plastic water distribution pipes," in [*National Research Council, Institute for Research in Construction*], (2000).

[9] Pure Technologies Ltd., "Purerobotics for water and wastewater pipelines." http://www.puretechnologiesltd.com/html/pure_robotics.php/ (2011).

[10] "ISM400 multimetric imote2 sensor board datasheet and user's guide." http://shm.cs.uiuc.edu/files/ISM400_Datasheet.pdf (June 2009).

[11] Yun, C. B., Sohn, H., Jung, H., Spencer, B., and Nagayama, T., "Wireless sensing technologies for bridge monitoring and assessment," in [*The Fifth International Conference on Bridge Maintenance, Safty and Management*], (July 11-15 2010).

[12] Tang, X., Liu, Y., Zheng, L., Ma, C., and Wang., H., "Leak detection of water pipeline using wavelet transform method," in [*International Conference on Environmental Science and Information Application Technology*], (2009).

[13] Chen, X.-j., Gao, Z.-f., Ma, Y.-e., and Guo, Q., "Application of wavelet analysis in vibration signal processing of bridge structure," in [*Int. Conf. on Measuring Technology and Mechatronics Automation*], (2010).

[14] "TMS570 microcontroller USB kit." http://focus.ti.com/docs/toolsw/folders/print/tmdx570ls20susb.html (February 2011).